Colloids and Surfaces B: Biointerfaces 159 (2017) 166–173

Contents lists available at ScienceDirect

Colloids and Surfaces B: Biointerfaces

journal homepage: www.elsevier.com/locate/colsurfb

Biomimetic Surfaces Supporting Dissociated Pancreatic Islet Cultures

Parker L. Andersen[a,b,c], Patrick Vermette[a,b,c,*]

[a] Laboratoire de bio-ingénierie et de biophysique de l'Université de Sherbrooke, Department of Chemical and Biotechnological Engineering, Université de Sherbrooke, 2500 boulevard de l'Université, Sherbrooke, Québec, J1K 2R1, Canada
[b] Institut de pharmacologie de Sherbrooke, Faculté de médecine et des sciences de la santé, 3001 12e Avenue Nord, Sherbrooke, Québec, J1H 5N4, Canada
[c] Research Centre on Aging, Institut universitaire de gériatrie de Sherbrooke, 1036 rue Belvédère Sud, Sherbrooke, Québec, J1H 4C4, Canada

ARTICLE INFO

Article history:
Received 21 April 2017
Received in revised form 20 July 2017
Accepted 24 July 2017
Available online 25 July 2017

Keywords:
Biomimetic surfaces
Carboxy-methyl-dextran
Islet cells
Insulin assay
Low-fouling surfaces

ABSTRACT

This study describes a method to screen biomimetic surfaces based on intracellular insulin content of either fully or partly dissociated primary endocrine islet tissue. It is challenging to maintain endocrine pancreatic islets and more so, dissociated ones. Physiological activity of isolated islet cells *in vitro* declines due to loss of cell-to-cell and cell-to-extracellular matrix interactions. An *in vitro* model was developed to evaluate specific extracellular binding components potentially affecting islet biology, with the intention to identify *in vivo*-like peptides promoting survival and function. Synthetic peptides were bound to low-fouling carboxy-methyl-dextran surfaces, effectively presenting defined surfaces while minimizing non-specific interactions. These biomimetic surfaces were screened based on intracellular insulin content of applied mouse primary islet tissue by analysis with an anti-insulin cell-ELISA. Three active biomimetic surfaces were identified, two laminin- (IKLLI and PDSGR) and one cadherin (HAVDI)-derived, which supported adhesion and survival of insulin-containing cultures for 5 days, respectively suggesting a benefit from both cell-extracellular matrix and cell–cell interactions. Cells from dissociated islets show progression over 10 days on the HAVDI-biomimetic for the insulin immunoreactivity and cell density. The three surfaces did not act additively or synergistically. A favorable reaction to glucose-stimulated insulin secretion on the cadherin-biomimetic indicated the cultures were physiologically functional. This supportive role of biomimetic peptides represents initial progress in defining minimal extracellular binding requirements influencing islet cell physiology. This will influence further optimization of growth surfaces and promote the basic understanding of islet biology. Low-fouling biomimetics are predicted to be applicable to additional diverse culture systems.

1. Introduction

The pancreas operates as a large exocrine organ containing discrete endocrine structures termed the 'Islets of Langerhans', which occupy a small percentage of the total pancreatic volume. The exocrine and endocrine tissues are each associated with ductal, vascular and neuronal systems [1]. The pancreatic extracellular matrix (ECM) is specialized in at least two locations proposed to directly affect islet cell biology, namely: 1) the peri-islet ECM, and 2) the intra-islet peri-vascular ECM. These ECMs, and specialized cell architectures, divide pancreatic secretions into two directions [1–4]. The exocrine-derived (digestive) pro-enzymes exit only through the ductal system, away from the islets and vasculature. Alternatively, the intra-islet peri-vascular ECM and associated capillary systems are specialized to monitor blood glucose levels, and immediately release hormones primarily (but not necessarily exclusively) into the blood circulation [1]. Circulating glucose concentration is balanced largely by the hormones glucagon (released from islet α-cells) and insulin (released from islet β-cells), respectively promoting glucose mobilization or storage by peripheral tissues. Adjacent β-cells are directly coupled by gap junctions, resulting in cooperative release of insulin [5]. Alternatively, α- and β-cells operate in a paracrine manner to reciprocally restrict hormone release [6,7]. Alpha and β-cells react to influences from many systems, including additional endocrine islet cell types, pancreatic exocrine tissue, various peripheral glands, circulating metabolites and neural systems [8–10]. Cooperation becomes most evident when islets are dispersed into single cells, resulting in reduced viability and/or insulin miss-regulation, which is partially reversible upon re-aggregation. [5,11,12]. Both ECMs and multiple cell–cell interactions are therefore predicted to be

* Corresponding author at: Department of Chemical and Biotechnological Engineering, Université de Sherbrooke, 2500 boul. de l'Université, Sherbrooke, Québec, J1K 2R1, Canada.
E-mail address: Patrick.Vermette@USherbrooke.ca (P. Vermette).

http://dx.doi.org/10.1016/j.colsurfb.2017.07.060
0927-7765/

required for islet cell physiological activity [13]. To our knowledge, no materials or surfaces allow long-term culture of functional primary cells from dissociated pancreatic islets.

The generalized structure of the islet ECMs (including peri-islet and vascular) comprises a basement membrane (consisting of non-fibrillar collagen IV, laminins, nidogens, proteoglycans and hyaluronan), with the addition of fibrous collagens (I, III and VI) in the peri-islet ECM [14,15]. Each of these components exhibit a large diversity due to variations in mRNA splice transcripts, alternative binding partners (*i.e.*, the various combinations of laminin α, β and γ chains) and post-translational/post secretion chemical modifications. These make the ECM heterogeneous between species, tissues, and specific localization [16,17]. To complicate matters, following insult most tissues undergo a damage response and remodel their environment significantly, most notably with: scar tissue formation involving alterations in residing cell populations (including inflammation), ECM deposition, and cell surface and/or secreted proteins which bind or modify the ECM. Damage/stress responses by islets have been described [18], including alterations in the islet ECM [19,20].

We hypothesized that the *in vitro* presence of defined surfaces derived from the *in vivo* pancreas ECM will enhance survival and function of dissociated islet tissue by supporting structural integrity. We therefore designed a model system consisting of defined peptide surfaces, to which primary mouse islet tissue was applied, to investigate potential ECM peptide effects. Potentially, islet cultures may respond to the isolation technique (involving both chemical and physical damage) with an innate damage response likely superior to what we as experimenters can produce. Peptide-bearing surfaces were derived from amino acid sequences believed to naturally occur within the pancreatic ECM associated with islets, or from peptide sequences derived from proteins between neighbouring islet cells (in this case cadherins), attached to carboxy-methyl-dextran (CMD) surfaces. When applied as a surface, CMD is nearly inert to protein adsorption, cell binding and most biological compounds [21,22]. In this report, we define a 'biomimetic' surface as 'a biomolecule attached to a low-fouling CMD surface'. Because insulin expression is one of the primary prerequisite for islet function, we screened multiple biomimetics by assaying intracellular insulin content of applied primary mouse islet tissue. The initial screen leads to further characterization of selected surfaces, including analysis by glucose-stimulated insulin secretion (GSIS) and changes in insulin content as cultures progressed. We propose low-fouling biomimetic application as a viable method to optimize and understand fundamentals of islet biology including a hypothesized intrinsic damage response.

2. Materials and methods

2.1. Production of low-fouling surfaces

Dextran was chemically modified to produce CMD [22]. Briefly, dextran (MW of approximately 64–76 kDa) from *Leuconostoc mesenteroides* (Sigma-Aldrich, D8821) was treated with bromoacetic acid, dialyzed extensively, lyophilized and stored at −20 °C. The percentage of carboxy-methylation, which forms the substrate for peptide application, was determined to be 29% by NMR spectroscopy (Supplemental Fig. 1) [23]. The application of CMD onto culture surfaces was modified from established procedures [22,24,25] with the utilization of reduced poly-L-lysine (PLL) as a linking mechanism as an alternative to amine-bearing surfaces produced by plasma polymerization. To tissue culture surfaces, PLL (MW of approximately 30–70 kDa, Sigma-Aldrich, P9155) was first applied overnight at a concentration of 0.1 mg/mL in water. Plates were washed 3 times with water and exposed to 2 mg/mL CMD plus 20 mM 1-ethyl-3-(3-dimethylaminopropyl) carbodiimide hydrochloride (EDC, Sigma-Aldrich, E1769) and 20 mM *N*-hydroxysuccinimide (NHS, Sigma-Aldrich, 130672) for 4 h, then washed with 1 M NaCl twice over 24 h, then 4 times with water over 24 h. CMD-coated surfaces were either washed 3 times over 30 min with serum-free growth medium immediately before culturing, or alternatively air dried for atomic surface analysis.

2.2. Production of biomimetic surfaces

Peptide application to low-fouling CMD surfaces has previously been described and exploited [21,22,26]. Attached biomolecules were short chains of amino acids (with and without linkers), full length proteins or recombinant fragments conjugated to a mussel adhesion protein derived from *Mytilus edulis* (MAPTrix). The peptides used to produce the biomimetics are detailed in Supplemental Table 1. To covalently link peptides and proteins, CMD-bound surfaces were pre-exposed to 200 mM EDC/200 mM NHS for 10 min, rinsed quickly with water 3 times (to avoid polymerization onto peptide carbohydrate groups) and exposed to 100 μg/mL of the desired peptide, rat tail type I collagen (Corning, 354236) or human fibronectin (Millipore, FC010), for 4 h. MAPTrix peptides were bound by direct adsorption based on the high-binding affinity of the linked mussel adhesion peptide. Biomimetic surfaces were either washed 3 times over 30 min with serum-free growth medium immediately before culturing, or alternatively air dried for atomic surface analysis.

2.3. Surface characterization by X-ray photoelectron spectroscopy (XPS)

Atomic characterization of surfaces was performed with an AXIS HS X-ray photoelectron spectrometer (Kratos Analytical, Manchester, UK), fitted with a monochromatic Al-Kα source of 225 W. Spectral surveys determined relative atomic carbon, nitrogen and oxygen composition (Supplemental Table 2), and high-resolution C 1 s spectral analysis identified the presence of carbon bonds (Supplemental Fig. 2) as detailed in online Supplemental Technical Notes.

2.4. Islet cultures

Adult CD-1 mice were euthanized by CO_2 asphyxiation as per local university animal ethical protocol #367-14. Pancreases were aseptically injected with 0.2 mg/mL type V collagenase (from *Clostridium histolyticum*, Sigma-Aldrich, C9263) in Dulbecco's modified Eagle's medium (DMEM, Sigma-Aldrich, D5523) plus 50% FBS (Gibco/Life Technologies, 12483-020), 25 μM *N*-acetyl-L-cysteine (Sigma-Aldrich, A9165), 100 mM nicotinamide, 15 mM HEPES and 4.2 mM $NaHCO_3$. All values are final working concentrations. Tissue was incubated for approximately 120 min at 37 °C, with trituration every 30 min. Non-digested tissue was further exposed to collagenase for an additional 15–30 min. The high FBS content was intended to minimize islet damage by contaminating proteases potentially activated from the exocrine tissue during isolation. Collagenase-released islets were pipette picked, rinsed with Hanks' balanced salt solution and dissociated at 37 °C in either Trypsin/EDTA (0.25%, Gibco/Life Technologies, 25200-056) for 5 min at 37 °C to disrupt islets into small clusters of cells, or Accutase (Millipore, SCR005) for 8–12 min into near single-cell populations (Supplemental Fig. 3). Islet cultures were routinely maintained in DMEM with 10% FBS containing 5.6 mM glucose, 15 mM HEPES, 100 mM nicotinamide, 25 μM *N*-acetyl-L-cysteine and 20 mM $NaHCO_3$ (to balance with a 5% CO_2 atmosphere). Glucose was kept at 5.6 mM to reflect physiological levels. Typically, islet cultures contained 10–15 dissociated islets per well and

generally resulted in significant cell density variances between dissections/islet isolations.

2.5. Cell line cultures

PANC-1, a human cancer derived ductal-like cell line, was obtained from ATCC (Manassas, Virginia, USA, CRL-1469). INS-1 cells, a rat β-like cell line, was obtained from AddexBio (San Diego, California, USA, C0018007). Both cell lines were cultured in DMEM with 5.6 mM glucose, 20 mM $NaHCO_3$ and 10% FBS, with the addition of 50 μM β-mercaptoethanol to INS-1 cultures. INS-1 cells were routinely cultured on surfaces pre-incubated overnight with 0.01 mg/mL PLL.

2.6. Insulin and cell density analysis

An established cell-ELISA procedure was used to measure relative intracellular insulin and relative cell density [27]. This procedure measures solute absorbance and therefore removes user bias from microscopic imaging. Briefly, cultures were grown in 96-well culture plates, modified with indicated biomimetic surfaces for the indicated durations, agitated for 8–10 s to suspend debris then immediately fixed for 30 min by adding freshly depolymerized paraformaldehyde in PBS added to the culture medium to a final concentration of 2%. All rinsing steps consisted of 7 rinses with PBS plus 0.025% Tween-20 (PBST) over 30 min. Brisk agitation was re-initiated beginning 10 min after the start of fixation and continued throughout the procedure. Cells were permeabilized with 0.5% Triton X-100 for 5 min (in the 2nd wash) and endogenous peroxidase quenched with 0.3% H_2O_2 for 5 min (in the 4th wash). Wells were filled with blocking solution consisting of 5% fat-free powdered milk in PBST for 1 h. A mouse horseradish peroxidase-conjugated anti-insulin antibody (Abcam, Ab28063, 1:2000) was applied for 1 h. Slowest kinetic rate TMB solution (Abcam, ab171527) was applied for 5 min and the reaction stopped by the addition of 1 N HCl and absorbances read at 450 nm (Synergy HT plate reader with Gen 5 software from Bio-Tek industrial, Vermont, USA). The identical cultures were subsequently exposed to 0.3% Janus Green B, which predominately stains nuclei of formaldehyde-fixed cells. Bound Janus Green B was released with 0.5 N HCl and absorbances read at 595 nm to indicate relative culture densities. This procedure gives a linear function of insulin content and cell density (Supplemental Fig. 4), dependent upon the number of surviving cells or tissue seeded per well [27].

2.7. Immunocytochemistry

Cultures were fixed, permeabilized and blocked. The primary antibodies: mouse anti-insulin (Abcam, ab9596, 1:400), rabbit anti-glucagon (Abcam, ab18461, 1:200) and rabbit anti-Ki67 (Abcam, ab16667, 1:400), were applied in blocking solution for 60 min. The secondary antibodies: goat anti-rabbit Alexa-488 (Molecular probes, 11034, 1:2000) and goat anti-mouse Alexa-555 (Molecular Probes, 21422, 1:2000), as well as Hoescht (2 μg/mL) were combined and applied for 30 min in blocking solution.

2.8. Glucose-stimulated insulin secretion (GSIS)

Cultures were gently, but quickly rinsed twice with a modified (for atmospheric CO_2) Krebs-Ringer buffer (25 mM HEPES, 115 mM NaCl, 4.2 mM $NaHCO_3$, 5 mM KCl, 1 mM $MgCl_2{\cdot}6H_20$, 5 mM $CaCl_2{\cdot}2H_2O$ and 0.1% BSA) containing 2.8 mM glucose, then 60 min for each sequential step: 2.8 mM glucose (twice), 28 mM glucose, 28 mM glucose + 50 μM isobutyl-methyl-xanthine (IBMX), 2.8 mM glucose and 28 mM glucose + 50 μM IBMX. All rinsings were done at 37 °C with gentle agitation. Culture supernatants were collected at selected time points and frozen at −20 °C for analysis using a commercial anti-insulin ELISA assay kit (ALPCO rat high range ELISA, INSRTH-E01).

2.9. Data and image analysis

Determination of means, standard deviations and R^2 values were calculated with Excel software (Microsoft Office 365). All images were captured using a Nikon inverted microscope (Nikon Eclipse TE2000-S) and images taken using a Zeiss AxioCam MRm camera with Zeiss AxioVision SE64 software. Color was added to fluorescent images with Photoshop software.

3. Results

3.1. Analysis of biomimetic surfaces

The surface composition of prepared surfaces were analyzed at the atomic level by XPS. Spectral survey determines relative atomic ratios of the elements, and high-resolution C 1 s spectral analysis identifies the presence of specific bonds (C—C and C—H at 285 eV, C—O at 286.6–286.9 eV, and O—C=O + peptide bonds at 288–289 eV) [25,28,29]. XPS analysis confirmed addition of CMD by the incorporation of carbon-bound oxygen (Supplemental Fig. 2 and Supplemental Table 2). PANC-1 cells were utilized for low-fouling characterization of the CMD surface, as they are highly adherent and relatively insusceptible to anoikis when allowed to form clusters in suspension, such as above CMD surfaces (Supplemental Fig. 5A). After being suspended over CMD for 3 days, the PANC-1 clusters were passaged onto normal culture surfaces, which allowed cell attachment and proliferation indicating CMD is non-toxic, at least to these cells (Supplemental Fig. 5B). To demonstrate temporal stability of CMD, poly-L-lysine was applied as 25 μL spots on culture dishes before application of EDC/NHS/CMD, which restricted CMD application to a defined and predicted pattern. PANC-1 cells were seeded and near-identical fields of interest were identified by blemishes on the surface, and occasionally photographed over a 14-day period (Supplemental Fig. 6). At the time of submission of this article, the only cells known by the authors to significantly bind CMD were peritoneal macrophages (Supplemental Fig. 7). The low-fouling properties of the CMD coatings have been well investigated and detailed characterization has been presented [21,22,24–26]. CMD surfaces are therefore considered low-fouling to most biomolecules and utilized further as a substrate to produce the biomimetics. Analysis of peptide binding by XPS analysis was inconclusive because of the residual presence of nitrogen on EDC/NHS-activated CMD (Supplemental Table 2). With the high C 1s analysis however, several applications suggested a modification whereas some peptide applications were inconclusive or negative. (Supplemental Fig. 2). The confirmation of bound peptide, given their small size, is therefore dependent upon biological activity.

3.2. Initial biomimetic screen with partially dissociated islets

Thirteen biomimetic surfaces were initially screened after trypsin-digested islets were applied for 5 days to quickly decide upon the most active surfaces for further investigation (Fig. 1). Four of the surfaces were expected to have no bioactivity, namely: CMD, EDC/NHS-activated CMD, the RGE-biomimetic (a presumably inactive form of RGD), and the HWRGWV-biomimetic (designed to bind the Fc portion of antibodies). Interestingly, with the PHSRN-RGDSP-biomimetic, culture density was augmented without a concurrent parallel insulin increase. Since insulin content is the primary prerequisite for islet function, this biomimetic was not investigated further. Most biomimetics exhibited insufficient insulin content to

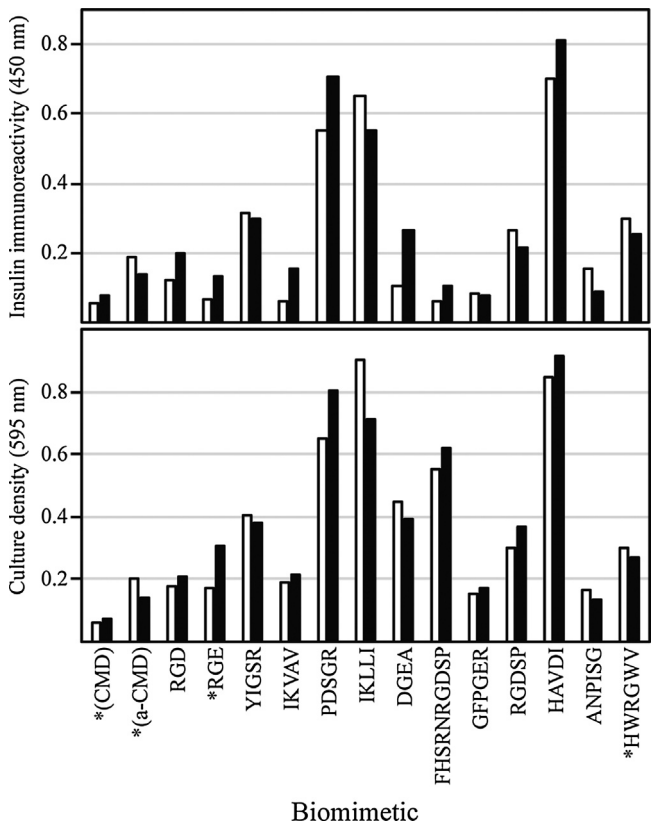

Fig. 1. Initial screen of biomimetic surfaces. Trypsin-digested islets were cultured on the indicated biomimetic surfaces for 5 days. The upper panel represents insulin content as measured by cell-ELISA. The lower panel represents corresponding culture densities as determined by the Janus Green B assay. Each bar represents a single well and each color (white or black) represents a single experiment. Asterisks denote surfaces predicted to have no cell binding capability. The term 'aCMD' refers to EDC/NHS-activated CMD.

warrant further investigation; only the PDSGR-, IKLLI- and HAVDI-biomimetics were selected for further investigation. Ineffective biomimetics were not characterized for viability or anoikis, as insulin expression was the priority. Also, although of great interest, characterization of complete islet cell activity was outside the scope of the present study.

3.3. Islet response to selected biomimetic surfaces

Islets were digested with either trypsin or Accutase® to respectively produce partially-dissociated or nearly-fully dissociated cell suspensions (Supplemental Fig. 3) and cultured on selected biomimetics for 5 days before analysis (Fig. 2). Cultures on PDSGR-, IKLLI- and HAVDI-biomimetics exhibited an insulin content which reflected cell density, whereas the CMD control remained virtually without cell attachment. During initial characterization of the surfaces, the β-like INS-1 cell line was utilized as a technically less demanding method to observe binding to biomimetic surfaces as opposed to islet tissue application. INS-1 cells responded to these biomimetics with binding and insulin expression. However, the insulin content in the N-terminal-linked IKLLI-biomimetic indicated an insulin content relative to cell density higher than that on the other two peptides (Supplemental Fig. 8). Because of the EDC/NHS activation of the CMD during peptide binding relies on the N-terminal amine of the peptide, there was the possibility that the terminal amine group of the lysine residue of IKLLI would act as a covalent modification site, potentially affecting peptide presentation. We therefore applied the same three peptides by C-terminal linkage to CMD by sulfo-EMS activation and repeated the assay with INS-1 cells resulting in cultures containing nearly equal insulin on each of the three biomimetics (Supplemental Fig. 9A). The differential expression of insulin in INS-1 cells is interesting and may warrant investigation in the future. However, the same reaction was not observed with dissociated islets (Supplemental Fig. 9B). We chose to continue with the more relevant primary tissue model system rather then the β-cell 'like' line.

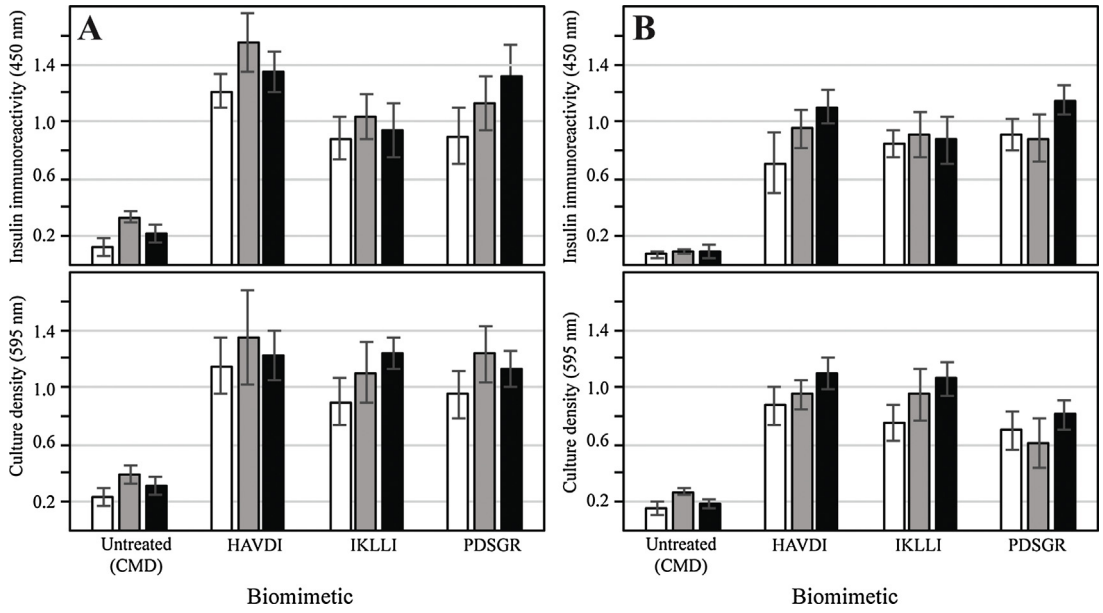

Fig. 2. Characterization of islet cultures on selected biomimetic surfaces. Islet preparations were cultured on the indicated biomimetic surfaces for 5 days. *A*: Analysis of trypsin-dissociated islets. *B*: Analysis of Accutase®-dissociated islets. Upper panels represent insulin content as measured by cell-ELISA. Lower panels represent corresponding culture densities as determined by the Janus Green B assay. Each bar color represents the averages of three individual experiments (3 experiments in '*A*' and three experiments in '*B*') to demonstrate variation between islet preparations. Error bars indicate standard deviations between three wells in each experiment.

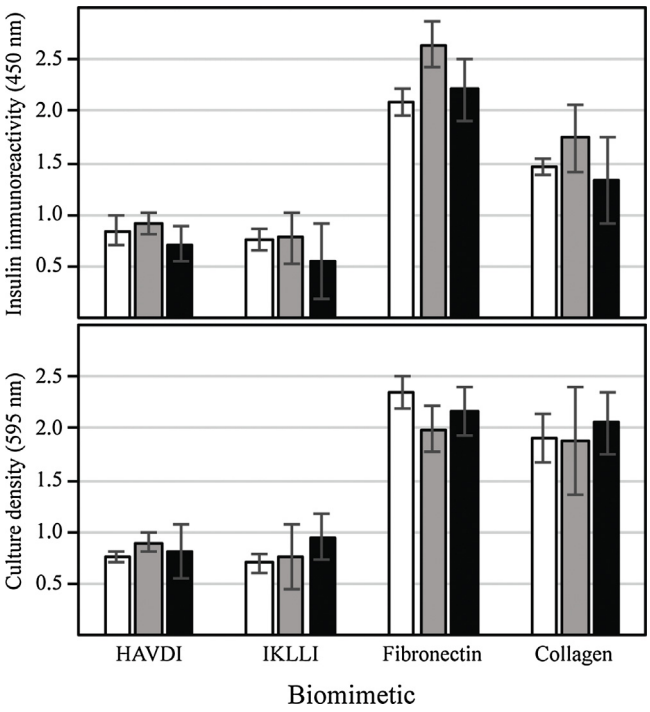

Fig. 3. Comparison of biomimetic surfaces with full length ECM molecules. Accutase® -dissociated islets were cultured on the indicated biomimetic surfaces and full-length biomolecules for 5 days. The upper panel represents insulin content as measured by cell-ELISA. The lower panel represents corresponding culture densities as determined by the Janus Green B assay. Each bar color represents the averages of three individual experiments to demonstrate variation between islet preparations. Error bars indicate standard deviations between three wells in each experiment.

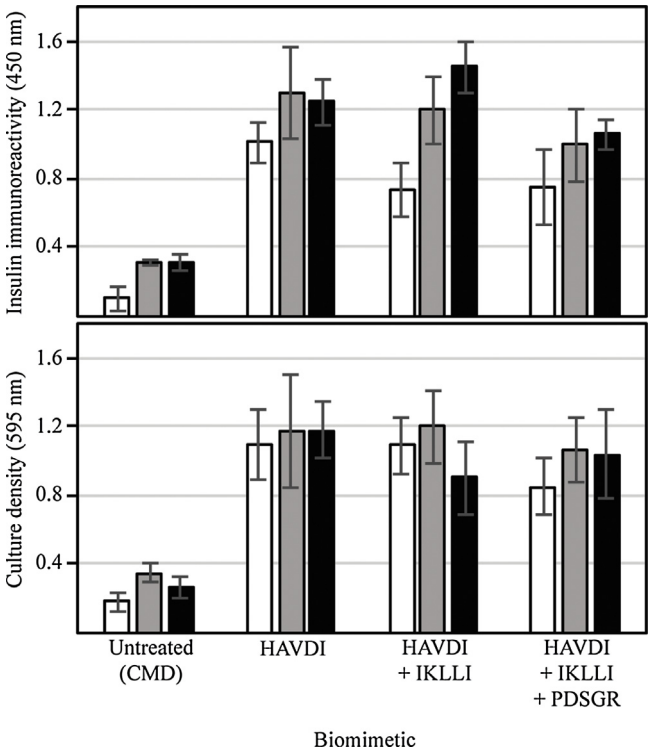

Fig. 4. Analysis of cooperative effects of biomimetic surfaces. Accutase® -dissociated islets were cultured on the indicated biomimetic surfaces for 5 days. The upper panel represents insulin content as measured by cell-ELISA. The lower panel represents corresponding culture densities as determined by the Janus Green B assay. Each bar color represents the averages of three individual experiments to demonstrate variation between islet preparations. Error bars indicate standard deviations between three wells in each experiment.

3.4. Biomimetic surfaces comparison to full length ECM proteins

Biomimetics were compared to surfaces coated with rat tail type I collagen and human serum-derived fibronectin *via* EDC/NHS-activated CMD. Accutase® -dissociated islets were cultured for 5 days on each surface. Comparing sister-cultures on biomimetic surfaces demonstrated lower insulin content and lower cell densities on the peptide mimetics relative to the full-length protein applications (Fig. 3). This suggests the peptides do not completely recapitulate the true ECM, which was not unexpected.

3.5. Dissociated islet response to combinations of biomimetic surfaces

ECM binding sites are expected to operate cooperatively and sometimes synergistically [30]. Because two of the active biomimetic surfaces are laminin-derived and one cadherin-derived, we sought to determine if these peptides operate in a cooperative manner. Upon combining the peptides (applied in an equimolar ratio), little differences were observed in insulin content nor cell density (Fig. 4), implying that the peptides merely promote binding and are non-instructive to influencing insulin content directly.

3.6. Progression of dissociated islet cultures on the HAVDI-biomimetic

The HAVDI-biomimetic was chosen for further characterization. Sister-cultures of Accutase® -dissociated islets on the HAVDI-biomimetics were analyzed for insulin content and cell density sequentially over several days. Cultures demonstrated a gradual increase in insulin content as the culture density increased over the culture period (Fig. 5). Analysis by anti-insulin and anti-glucagon immunocytochemistry indicated the presence of α/β-cell aggregates (Supplemental Fig. 10), suggesting restoration and/or maintenance of intrinsic islet cell–cell interactions, and an overall well-being of the culture.

3.7. Physiological activity on the HAVDI-biomimetic

HAVDI-biomimetic surfaces were analyzed for supporting physiological activity (Fig. 6). Accutase® -dissociated islets were cultured on the HAVDI-biomimetics for five days then analyzed for GSIS. Cultures taken from an initial low-glucose concentration (2.8 mM) to a high-glucose concentration, as expected, increased insulin release into the culture medium, which was augmented by the presence of IBMX. Importantly, this was reversible as demonstrated by lowering glucose and re-applying a high concentration of glucose (with IBMX), confirming a physiological response and not an artifact of cell lysis inadvertently increasing soluble insulin. This indicates Accutase® -dissociated islet cultures on the HAVDI-biomimetics are physiologically relevant.

4. Discussion

Traditionally, heptylamine application by plasma polymerization vacuum chemistry has been used as a chemical linker to immobilize CMD [21]. Unfortunately, plasma chemistry is specialized, technically demanding and limited to relatively few laboratories. This technical limitation was overcome here by the utilization of poly-L-lysine adsorption replacing plasma deposition of *n*-heptylamine. Immobilization of CMD was confirmed by XPS analysis (observed as an increase in carbon-bound oxygen), and low-fouling activity confirmed by loss of cell binding and ingrowth.

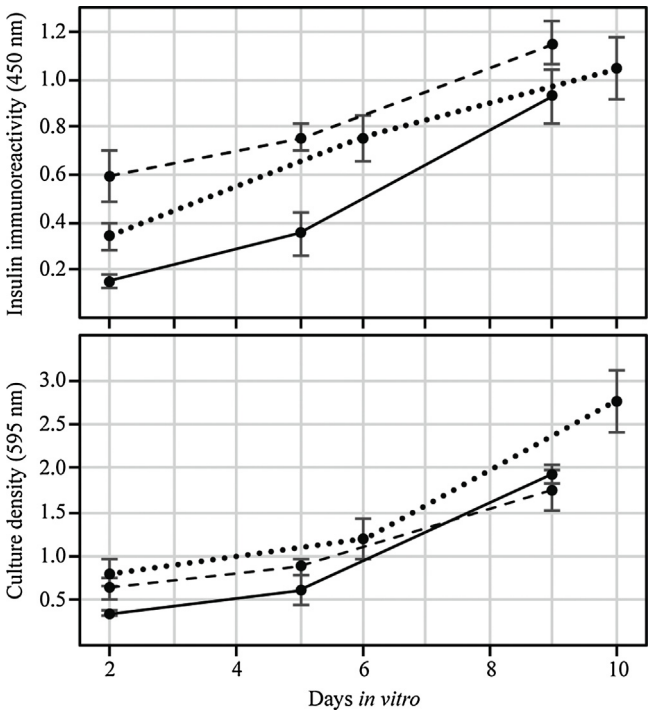

Fig. 5. Islet culture progression over 10 days on the HAVDI-biomimetic. Accutase® -dissociated islets were cultured on HAVDI-biomimetic surfaces and analyzed at the indicated time points. The upper panel represents insulin content as measured by cell-ELISA. The lower panel represents corresponding culture densities as determined by the Janus Green B assay. Each type of line (dotted, dashed and solid) represents the averages of three individual experiments to demonstrate variation between islet preparations. Error bars indicate standard deviations between three wells in each experiment.

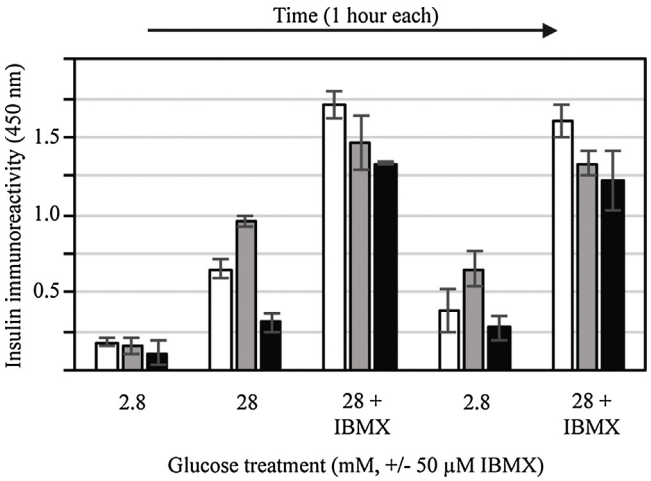

Fig. 6. Functional analysis of islet cultures on the HAVDI-biomimetic. Accutase® -dissociated islets were cultured on HAVDI-biomimetic surfaces for 5 days and subjected to the indicated glucose concentrations (+/− IBMX) in succession, for 1 h each. Immunoreactivity (raw absorbance) represents relative insulin content. Each bar color represents the averages of three individual experiments to demonstrate variation between islet preparations. Error bars indicate standard deviations between three wells in each experiment.

The use of poly-L-lysine (at 10 times the concentration used here) for CMD immobilization has been described in the past exhibiting low-fouling success [25]. The advantage of using poly-L-lysine therefore renders the CMD-based low-fouling technique applicable to any basic cell biology laboratory, without the requirement for plasma vacuum chemistry. The technique is therefore predicted to be applicable for alternative (non-islet) models, such as cell-migration and process extension investigations (with caution, Supplemental Fig. 7).

However, we cannot assume the surfaces have not been further modified by the applied cells (or serum), nor if applied cells have reacted to the CMD. The use of serum in the cultures can affect the biological properties of surfaces, and may modify/affect the low-fouling properties of any surfaces. However, the fouling resistance of CMD layers toward serum has been demonstrated [31]. The observation of macrophages and the mussel-adhesion protein (with the PHSRN-RGDSP-biomimetic as an example) attaching to CMD supports the notion that these surfaces are not completely inert. Nevertheless, because the bare CMD surfaces, used as controls here, remained low-fouling for up to 14 days with a cell line known to have a good capacity to adhere allows discriminating the effect of the immobilized peptides and proteins. Although the presence of serum and/or additional cells are expected to affect cellular activity, possibly by providing unidentifiable protein linkages between the applied peptides and cell surface receptors, as one possible example, the presented cultures are dependent upon the prior peptide application to the low-fouling CMD coating. The involvement of extraneous factors will never be eliminated. Therefore, the use of CMD low-fouling surfaces to validate the bioactivity of the ECM peptides is justified here, to limit and delay non-specific interactions.

By XPS analysis, confirmation of peptide binding was inconclusive, giving their small size. High-resolution spectra and atomic nitrogen differences between CMD and biomimetics were observed, suggesting the presence of peptide bonds. The EDC/NHS/CMD activation intermediate is expected to be labile [32], but because of the observed presence of nitrogen on activated CMD, identification of peptide application is lacking. The expected highly charged CMD physically extending the structure may have also superseded peptide identification. However, XPS analysis does suggest the persistence of CMD surfaces following peptide application, which validates the low-fouling method (with the exception of the DGEA biomimetic application). Biomimetics are designed as short peptides. Additional higher order structures, modifications and codependent molecules are lacking unless provided during culture. We therefore cannot conclude if applied peptides, when bound to CMD, were physically presented to resemble native conformation. As such, identification of active biomimetics is dependent upon function (cell-binding/insulin content) and inactive biomimetics may be 'out of context' in this system, but not necessarily non-physiologically relevant. Therefore, inactive sequences may have been overlooked in the original screen.

The use of biomolecules for islet culture and implantation is not a novel idea. Isolation and dispersion of islets results in loss of ECM, vasculature, and all extra-islet influences, ultimately affecting islet viability and insulin expression/regulation [11,33–35]. This can be partially reversed experimentally by replacing cell-to-cell and cell-to-ECM interactions [13,36–40]. Many ECM components have been shown to affect islet cell biology, including various combinations of laminin chains [37], collagens [41], cadherins [39,40], Matrigel [33,42], fibronectin [43], and several short peptides [21,44–47]. A limitation of these experiments is that even when the culture is functional (supporting viability and a positive GSIS reaction), the biomolecules may be poorly defined chemically, and expected to be complex making interpretation difficult. Characterization of Matrigel has disclosed great complexity with in excess of 1800 proteins, with significant variation between preparations [48]. An advantage of the biomimetic system is that the applied biomolecules are nearly chemically defined, at least on initial application. The biomimetic surfaces are therefore considered a minimal starting point with an obvious importance of further optimization.

Culturing on the HAVDI-biomimetic demonstrated small clusters consisting of glucagon- and insulin-containing cells, as well as unidentified cells within and distinct from the clusters. Through the culture period, there was a gradual rise in insulin content, and the cultures responded favorably in the GSIS assay. The augmentation of the glucose response with IBMX is significant because it infers the involvement of an intracellular second messenger influence on insulin release, suggesting a physiological interaction with non-β accessory cells [12,13,49,50]. When cultures were co-stained for anti-Ki67 as a proliferation marker, we made the casual observation that Ki-67 positive cells did not co-localize to cells with either insulin- or glucagon-expressing cells, which gave us the impression α/β-cells were not active in the cell division cycle. The proliferating cells were not identified, and the total number and relative ratios of α- and β-cells were not determined due to significant variances between fields of view. Because adult tissue was used, and the culture time relatively short, it would be unexpected that β-cells are proliferating, or that non-β-cells began expressing insulin. This suggests the insulin content of surviving β-cells increases over time on the HAVDI-biomimetic, supporting a positive damage response by the islet cells.

It has previously been suggested that cell–cell contact and/or surface contact will influence hormone content and release [51], which coincides with results here. It is important to note that Accutase® is expected to contain many uncharacterized enzymes, which does not allow for prediction of acute cell-surface modifications (such as receptor elimination) of digested cell surfaces, therefore ECM receptors may need to be replenished by the cell for binding activity. Because the presence of cells not expressing insulin or glucagon was observed on the HAVDI-biomimetic, we cannot conclude the surface is specific for a specific cell type. The possibility exists that one cell directly promotes binding of another by physical contact, or modifies the surface promoting another's attachment indirectly. Importantly, the observation of a high culture density on the PHSRN-RGDSP-biomimetic without an apparent increase in insulin suggests biomimetic cell-panning is feasible. Combined, this indicates the well-being of the culture, and suggests that islet cells have an inherent capacity to respond to isolation-derived damage (chemical and physical), as is expected to happen during experimental and clinical procedures. Biomimetic peptides on low-fouling surfaces therefore provide a unique opportunity to investigate specific influences on islet cell biology.

The limiting factors for this project was the number/quality of islets procured from each dissection (producing variations between experiments as witnessed from comparing control raw absorbance values of the assays from different experiments), and the financial burden of the peptides. Regardless, this project has initiated a functional assay for further biomimetic characterization with applications to specific questions. This study presents an important application of biomimetic surfaces. The biomimetic surfaces developed here have a particular relevance to the medical, pharmaceutical, and biotechnological fields, as we are not aware that existing materials and surfaces do allow long-term culture of dissociated islets. The lack of proper materials and surfaces to support the viability and function of primary cells from islets limits the uses of these cells in transplantation and, in drug testing for the pharmaceutical industry, as well as it hinders their large-scale culture.

Acknowledgments

The authors thank the members of Vermette's laboratory including Tim Spitters, Rajesh Guruswamy Damodaran, Jamie Sharp, Sylvain Vigier, Vivian Lehmann and Evan Dubiel for helpful thoughts and discussions. We are also grateful for Sonia Blais for XPS analysis, Chantal Nadeau for animals caring, Samuel Aubert-Nicol of the local Chemistry Department (Univ. de Sherbrooke) for NMR analysis, and various members of the 'Boston Ithaca Islet Club' for advice on dissociating islets.

PV designed the concept of the project. PLA devised and performed the experiments, and wrote the initial manuscript. PV edited the manuscript. PLA and PV reciprocally argued until the final manuscript was decided upon.

PLA is the guarantor of this work and, as such, had full access to all the data in the study and takes responsibility for the integrity of the data and the accuracy of the data analysis.

The authors declare that no conflicts exist.

Funding was provided by the Quebec Consortium for Drug Discovery (CQDM) awarded to PV.

Appendix A. Supplementary data

Supplementary data associated with this article can be found, in the online version, at http://dx.doi.org/10.1016/j.colsurfb.2017.07.060.

Supplementary data is presented in this document directly following the references

References

[1] N. Ashizawa, T. Sakai, T. Yoneyama, Y. Kinoshita, Cellular arrangement of endocrine and exocrine glands in rat pancreas: interface between Langerhans islets and pancreatic exocrine glands, Pancreas 45 (2016) e48–50.
[2] O. Cabrera, D.M. Berman, N.S. Kenyon, C. Ricordi, P.O. Berggren, A. Caicedo, The unique cytoarchitecture of human pancreatic islets has implications for islet cell function, Proc. Natl. Acad. Sci. U. S. A. 103 (2006) 2334–2339.
[3] J.T. Low, M. Zavortink, J.M. Mitchell, W.J. Gan, O.H. Do, C.J. Schwiening, H.Y. Gaisano, P. Thorn, Insulin secretion from beta cells in intact mouse islets is targeted towards the vasculature, Diabetologia 57 (2014) 1655–1663.
[4] E. Geron, S. Boura-Halfon, E.D. Schejter, B.Z. Shilo, The edges of pancreatic islet beta cells constitute adhesive and signaling microdomains, Cell Rep. (2015) 317–325.
[5] R.K. Benninger, D.W. Piston, Cellular communication and heterogeneity in pancreatic islet insulin secretion dynamics, Trends Endocrinol. Metab. 25 (2014) 399–406.
[6] B. Hellman, A. Salehi, E. Gylfe, H. Dansk, E. Grapengiesser, Glucose generates coincident insulin and somatostatin pulses and antisynchronous glucagon pulses from human pancreatic islets, Endocrinology 150 (2009) 5334–5340.
[7] C. Kelly, N.H. McClenaghan, P.R. Flatt, Role of islet structure and cellular interactions in the control of insulin secretion, Islets 3 (2011) 41–47.
[8] D. Eberhard, E. Lammert, The pancreatic beta-cell in the islet and organ community, Curr. Opin. Genet. Dev. 19 (2009) 469–475.
[9] P. Meda, Protein-mediated interactions of pancreatic islet cells, Scientifica (Cairo) 2013 (2013) 621249.
[10] E. Bertelli, M. Bendayan, Association between endocrine pancreas and ductal system. More than an epiphenomenon of endocrine differentiation and development? J. Histochem. Cytochem. 53 (2005) 1071–1086.
[11] D. Salomon, P. Meda, Heterogeneity and contact-dependent regulation of hormone secretion by individual B cells, Exp. Cell Res. 162 (1986) 507–520.
[12] D.G. Pipeleers, F.C. Schuit, P.A. in't Veld, E. Maes, E.L. Hooghe-Peters, M. Van de Winkel, W. Gepts, Interplay of nutrients and hormones in the regulation of insulin release, Endocrinology 117 (1985) 824–833.
[13] D. Pipeleers, P.A. in't Veld, E. Maes, M. Van de Winkel, Glucose-induced insulin release depends on functional cooperation between islet cells, Proc. Natl. Acad. Sci. U. S. A. 79 (1982) 7322–7325.
[14] E. Korpos, N. Kadri, R. Kappelhoff, J. Wegner, C.M. Overall, E. Weber, D. Holmberg, S. Cardell, L. Sorokin, The peri-islet basement membrane, a barrier to infiltrating leukocytes in type 1 diabetes in mouse and human, Diabetes 62 (2013) 531–542.
[15] S.J. Hughes, A. Clark, P. McShane, H.H. Contractor, D.W. Gray, P.R. Johnson, Characterisation of collagen VI within the islet-exocrine interface of the human pancreas: implications for clinical islet isolation? Transplantation 81 (2006) 423–426.
[16] C. Frantz, K.M. Stewart, V.M. Weaver, The extracellular matrix at a glance, J. Cell Sci. 123 (2010) 4195–4200.
[17] J.C. Stendahl, D.B. Kaufman, S.I. Stupp, Extracellular matrix in pancreatic islets: relevance to scaffold design and transplantation, Cell Transplant. 18 (2009) 1–12.
[18] V. Cigliola, F. Thorel, S. Chera, P.L. Herrera, Stress-induced adaptive islet cell identity changes, Diabetes Obes. Metab. 18 (Suppl. 1) (2016) 87–96.
[19] R.L. Hull, M. Bogdani, N. Nagy, P.Y. Johnson, T.N. Wight, Hyaluronan a mediator of islet dysfunction and destruction in diabetes? J. Histochem. Cytochem. 63 (2015) 592–603.
[20] R. Vracko, Basal lamina layering in diabetes mellitus. Evidence for accelerated rate of cell death and cell regeneration, Diabetes 23 (1974) 94–104.

[21] E. Monchaux, P. Vermette, Bioactive microarrays immobilized on low-fouling surfaces to study specific endothelial cell adhesion, Biomacromolecules 8 (2007) 3668–3673.
[22] E. Monchaux, P. Vermette, Cell adhesion resistance mechanisms using arrays of dextran-derivative layers, J. Biomed. Mater. Res. 85A (2007) 1052–1063.
[23] F.F.-L. Ho, D.W. Klosiewicz, Proton nuclear magnetic resonance spectrometry for determination of substituents and their distribution in carboxymethylcellulose, Anal. Chem. 52 (1980) 913–916.
[24] D. Boutin, Y. Martin, P. Vermette, Study of the effect of process parameters for n-heptylamine plasma polymerization on final layer properties, Thin Solid Films 515 (2007) 6844–6852.
[25] K.M. McLean, G. Johnson, R.C. Chatelier, G.J. Beumer, J.G. Steele, H.J. Griesser, Method of immobilization of carboxymethyl-dextran affects resistance to tissue and cell colonization, Colloids Surf. B Biointerfaces 18 (2000) 221–234.
[26] E.A. Dubiel, C. Kuehn, R. Wang, P. Vermette, In vitro morphogenesis of PANC-1 cells into islet-like aggregates using RGD-covered dextran derivative surfaces, Colloids Surf. B Biointerfaces 89 (2012) 117–125.
[27] P.L. Andersen, P. Vermette, Intracellular insulin quantification by cell-ELISA, Exp. Cell Res. 347 (2016) 14–23.
[28] J.S. Stevens, S.L.M. Schroeder, Quantitative analysis of saccharides by X-ray photoelectron spectroscopy, Surf. Interface Anal. 41 (2009) 453–462.
[29] J.S. Stevens, A.C. de Luca, M. Pelendritis, G. Terenghi, S. Downes, S.L.M. Schroeder, Quantitative analysis of complex amino acids and RGD peptides by X-ray photoelectron spectroscopy (XPS), Surf. Interface Anal. 45 (2013) 1238–1246.
[30] S. Aota, M. Nomizu, K.M. Yamada, The short amino acid sequence Pro-His-Ser-Arg-Asn in human fibronectin enhances cell-adhesive function, J. Biol. Chem. 269 (1994) 24756–24761.
[31] J. Dubois, C. Gaudreault, P. Vermette, Biofouling of dextran-derivative layers investigated by quartz crystal microbalance, Colloids Surf. B Biointerfaces 71 (2009) 293–299.
[32] G.T. Hermanson, Bioconjugate Techniques, Acdemic Press, Inc., San Diego, California, 1996.
[33] C. Oberg-Welsh, Long-term culture in matrigel enhances the insulin secretion of fetal porcine islet-like cell clusters in vitro, Pancreas 22 (2001) 157–163.
[34] R.N. Wang, L. Rosenberg, Maintenance of beta-cell function and survival following islet isolation requires re-establishment of the islet-matrix relationship, J. Endocrinol. 163 (1999) 181–190.
[35] A. Lukinius, L. Jansson, O. Korsgren, Ultrastructural evidence for blood microvessels devoid of an endothelial cell lining in transplanted pancreatic islets, Am. J. Pathol. 146 (1995) 429–435.
[36] D. Bosco, L. Orci, P. Meda, Homologous but not heterologous contact increases the insulin secretion of individual pancreatic B-cells, Exp. Cell Res. 184 (1989) 72–80.
[37] G. Nikolova, N. Jabs, I. Konstantinova, A. Domogatskaya, K. Tryggvason, L. Sorokin, R. Fassler, G. Gu, H.P. Gerber, N. Ferrara, D.A. Melton, E. Lammert, The vascular basement membrane: a niche for insulin gene expression and Beta cell proliferation, Dev. Cell 10 (2006) 397–405.
[38] T. Otonkoski, M. Banerjee, O. Korsgren, L.E. Thornell, I. Virtanen, Unique basement membrane structure of human pancreatic islets: implications for beta-cell growth and differentiation, Diabetes Obes. Metab. 10 (Suppl. 4) (2008) 119–127.
[39] D. Bosco, D.G. Rouiller, P.A. Halban, Differential expression of E-cadherin at the surface of rat beta-cells as a marker of functional heterogeneity, J. Endocrinol. 194 (2007) 21–29.
[40] G. Parnaud, C. Gonelle-Gispert, P. Morel, L. Giovannoni, Y.D. Muller, R. Meier, S. Borot, T. Berney, D. Bosco, Cadherin engagement protects human beta-cells from apoptosis, Endocrinology 152 (2011) 4601–4609.
[41] T. Kaido, M. Yebra, V. Cirulli, A.M. Montgomery, Regulation of human beta-cell adhesion, motility, and insulin secretion by collagen IV and its receptor alpha1beta1, J. Biol. Chem. 279 (2004) 53762–53769.
[42] R. Perfetti, T.E. Henderson, Y. Wang, C. Montrose-Rafizadeh, J.M. Egan, Insulin release and insulin mRNA levels in rat islets of Langerhans cultured on extracellular matrix, Pancreas 13 (1996) 47–54.
[43] G. Chi-Rosso, P.J. Gotwals, J. Yang, L. Ling, K. Jiang, B. Chao, D.P. Baker, L.C. Burkly, S.E. Fawell, V.E. Koteliansky, Fibronectin type III repeats mediate RGD-independent adhesion and signaling through activated beta1 integrins, J. Biol. Chem. 272 (1997) 31447–31452.
[44] A. Llacua, B.J. de Haan, S.A. Smink, P. de Vos, Extracellular matrix components supporting human islet function in alginate-based immunoprotective microcapsules for treatment of diabetes, J. Biomed. Mater. Res. A 104 (2016) 1788–1796.
[45] D.J. Lim, S.V. Antipenko, J.M. Anderson, K.F. Jaimes, L. Viera, B.R. Stephen, S.M. Bryant, B.D. Yancey, K.J. Hughes, W. Cui, J.A. Thompson, J.A. Corbett, H.W. Jun, Enhanced rat islet function and survival in vitro using a biomimetic self-assembled nanomatrix gel, Tissue Eng. Part A 17 (2011) 399–406.
[46] C. Kuehn, E.A. Dubiel, G. Sabra, P. Vermette, Culturing INS-1 cells on CDPGYIGSR-, RGD- and fibronectin surfaces improves insulin secretion and cell proliferation, Acta Biomater. 8 (2012) 619–626.
[47] C.C. Lin, K.S. Anseth, Glucagon-like peptide-1 functionalized PEG hydrogels promote survival and function of encapsulated pancreatic beta-cells, Biomacromolecules 10 (2009) 2460–2467.
[48] C.S. Hughes, L.M. Postovit, G.A. Lajoie, Matrigel: a complex protein mixture required for optimal growth of cell culture, Proteomics 10 (2010) 1886–1890.
[49] S. Seino, H. Takahashi, W. Fujimoto, T. Shibasaki, Roles of cAMP signalling in insulin granule exocytosis, Diabetes Obes. Metab. 11 (Suppl. 4) (2009) 180–188.
[50] X. Jia, J.C. Brown, P. Ma, R.A. Pederson, C.H. McIntosh, Effects of glucose-dependent insulinotropic polypeptide and glucagon-like peptide-I-(7-36) on insulin secretion, Am. J. Physiol. 268 (1995) E645–651.
[51] G.C. Weir, P.A. Halban, P. Meda, C.B. Wollheim, L. Orci, A.E. Renold, Dispersed adult rat pancreatic islet cells in culture: A, B, and D cell function, Metabolism 33 (1984) 447–453.

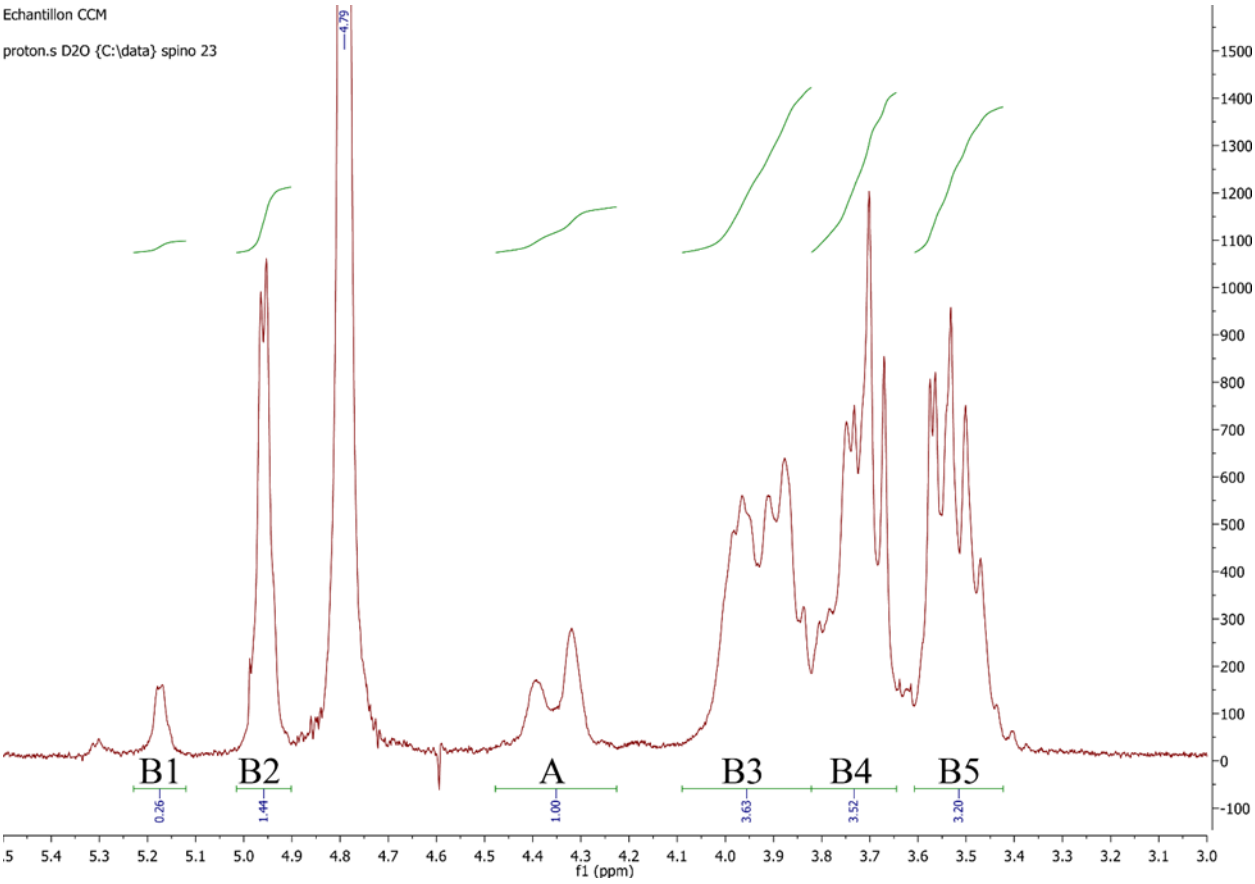

Supplemental Figure 1 - Determination of the degree of carboxymethylation of CMD. The degree of carboxylation was obtained from the ratio based on Ho and Klosiewicz (1980), as determined from the integrations shown, and calculated as described below.

$$\% \text{ carboxylation} = \{(A/2) / [(B1 + B2) + (B3 + B4 + B5)/6]/2\} \times 100$$
$$= \{(1/2) / [(0.26 + 1.44) + (3.63 + 3.52 + 3.20)/6]2\} \times 100$$
$$= 29\%$$

Supplemental Table 1 - Summary of peptides used in this study.

Target	Full construct*†	Origin	Supplier	Cat. number
RGD	GRGDS	Various	American peptide	44-0-23
RGE	RGE	--	American peptide	44-0-51
YIGSR	(Mussel adhesion protein)-YIGSR	Laminin	Sigma-Aldrich	164142K
IKVAV	(Mussel adhesion protein)-IKVAV	Laminin	Sigma-Aldrich	162242K
PDSGR	GPDSGRGGS	Laminin	American peptide	373335
IKLLI	GIKLLIGGC	Laminin	American peptide	373336
DGEA	(Mussel adhesion protein)-DGEA	Collagen	Sigma-Aldrich	165062K
PHSRN-RGDSP	(Mussel adhesion protein)-PHSRN-RGDSP	Fibronectin	Sigma-Aldrich	161252K
GFPGER	(Mussel adhesion protein)-GFPGER	Collagen	Sigma-Aldrich	165042K
RGD	GRGDSPC	Various	American peptide	44-0-25
HAVDI	GHAVDIGGS	Cadherin	American peptide	373333
ANPISG	GINPISGGGC	Cadherin	American peptide	373334
HWRGWV	(Mussel adhesion protein)-HWRGWV	Fc receptor binding peptide	Sigma-Aldrich	169841

* The target sequences are underlined.

† The 'Mussel adhesion protein' refers to commercial recombinant constructs (MAPTrix™) designed to link the muscle adhesion protein in frame with the target sequences of interest.

Supplemental Table 2 - Atomic composition of biomimetic surfaces as analyzed by XPS.

Surface	*Oxygen	*Carbon	*Nitrogen	C:O ratios	N:C ratios	N:O ratios
Plastic	13.06	86.57	.37	0.15	0.0043	0.028
Poly-L-lysine	9.62	87.48	2.89	0.11	0.033	0.30
CMD	15.17	81.83	2.46	0.19	0.030	0.16
†aCMD	16.1	80.44	3.4	0.20	0.042	0.21
GFPGER	16.53	79.78	3.39	0.21	0.042	0.20
DGEA	12.03	86.52	1.13	0.14	0.013	0.094
IKLLI	17.85	76.48	5.57	0.23	0.073	0.31
PHSRN-RGDSP	16.04	80.05	3.91	0.20	0.049	0.24
RGD	16.68	80.36	2.8	0.21	0.035	0.17
RGE	16.25	80.05	3.7	0.20	0.046	0.23
PDSGR	18.48	76.73	4.61	0.24	0.060	0.25
HAVDI	16.73	77.6	5.57	0.22	0.072	0.33

*Values are in percentages.

† The term ‘aCMD’ refers to EDC/NHS-activated CMD.

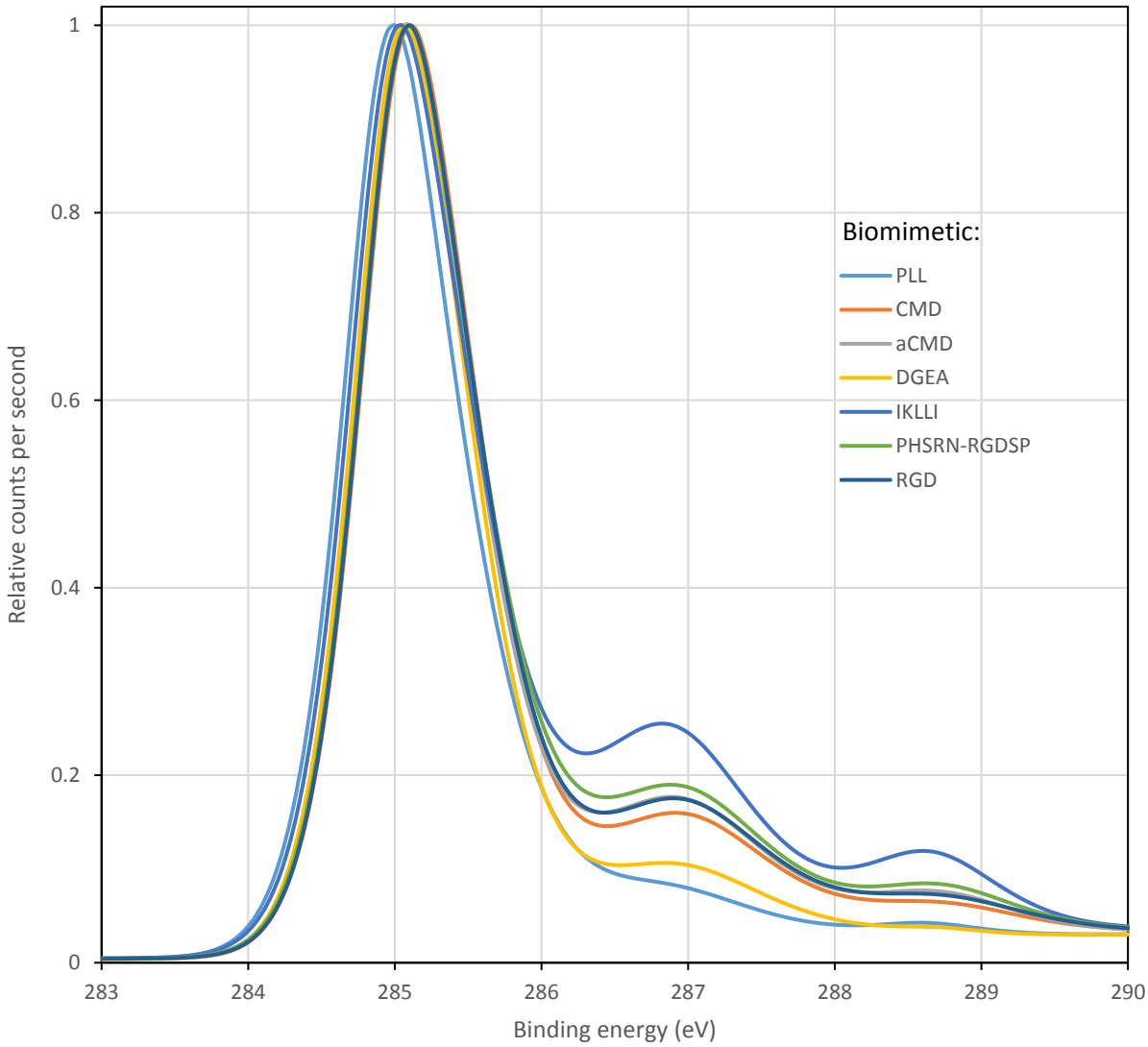

Supplemental Figure 2 - High resolution XPS C 1s spectra of selected surfaces normalized to the C-C/C-H peak. Carbon peaks are expected to occur at 285 eV (C-C and C-H_X), 286.6-286.9 eV (C-O), and 288-289 eV (O-C=O and peptide bonds). The term 'aCMD' refers to EDC/NHS-activated CMD. The RGD-biomimetic overlaps with the aCMD plot. The DGEA construct appeared to not bind and is more representative of the Poly-L-lysine (PLL) spectrum.

Supplemental note – Surface analysis by XPS.

X-ray photoelectron spectral analysis was performed with a Kratos AxisUltra DLD fitted with a monochromatic Al K(α) as the X-ray source (Kratos Analytical, Manchester, UK). Power was set at 140 W with a pass energy of 160 eV for survey scans, and at 225 W with pass energy of 20 eV for high resolution C 1s spectra. A pressure of 1×10^{-9} Torr was maintained. Following ISO 15472 procedure, the instrument work function was calibrated to give a binding energy of 83.96 eV for the Au 4f7/2 line for metallic gold, and the spectrometer dispersion was adjusted to give a binding energy of 932.62 eV for the Cu 2p3/2 line of metallic copper. Analysis areas were ovals of 300 x 700 microns. Samples were not grounded. The Kratos charge neutralizer system was used and deemed effective by monitoring the C 1s signal. Spectra were charge-corrected to C-C/C-H as the main peak of C 1s at 285 eV. Pre-analysis scans were compared with five post-analysis scans and a perfect fit of the data was obtained using CasaXPS version 2.3.16 as curve-fitting software. For carbon analysis, a single peak (70% Gaussian/30% Lorentzian) was used. Shirlex software was used for background curve-fitting.

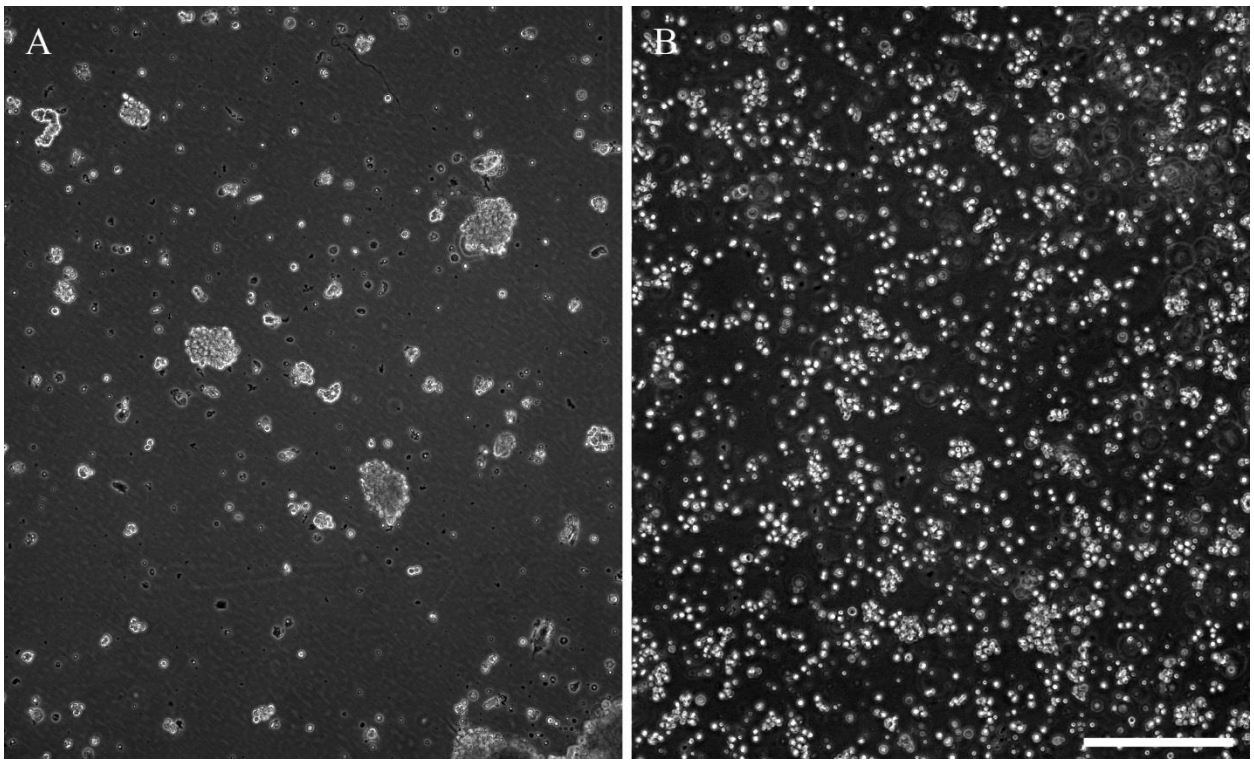

Supplemental Figure 3 - Appearance of islets following digestion. ***A*:** Phase contrast image of islets dissociated with trypsin. ***B*:** Phase contrast image of islets digested with Accutase®. Bar = 250 μm.

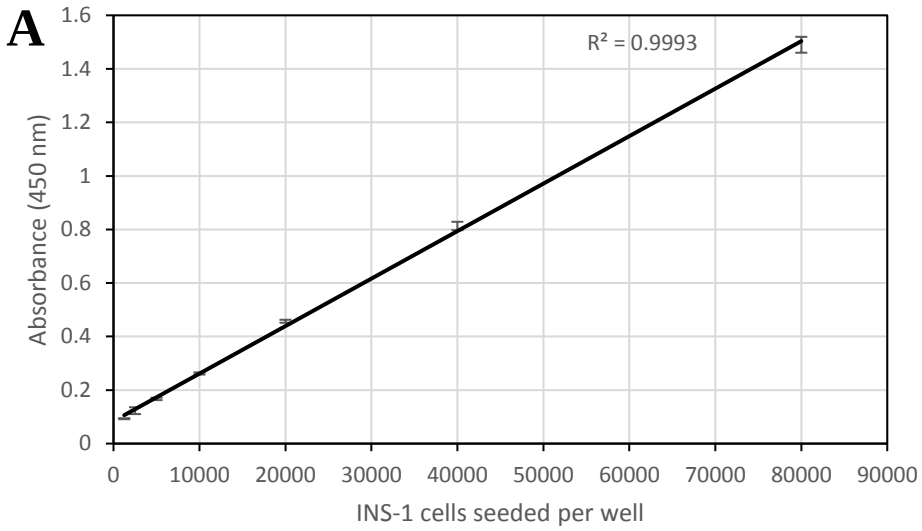

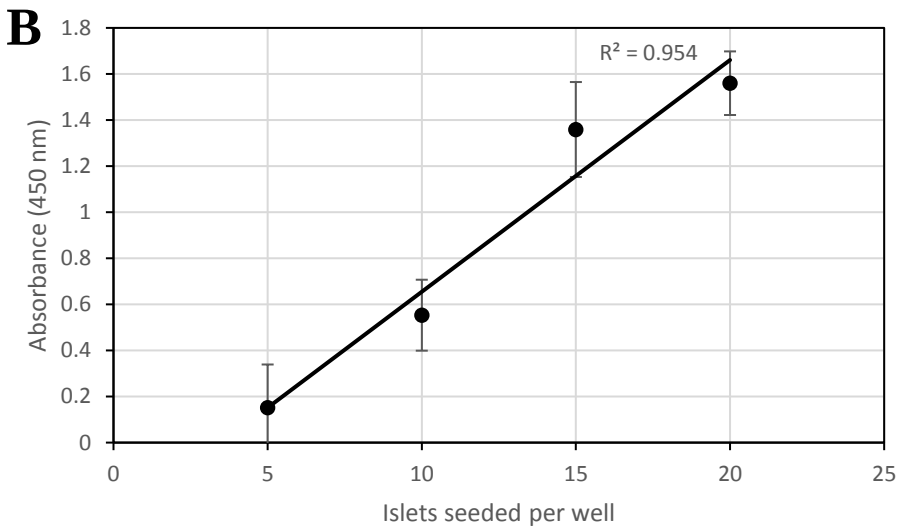

Supplemental Figure 4 - Linearity of insulin content as measured by cell-ELISA. ***A*****:** INS-1 cells were seeded overnight at the indicated densities. ***B*****:** Partially dissociated islets were cultured for 2 days at the approximate numbers of islet indicated. Absorbance at 450 nm represents insulin immunoreactivity. Statistical R^2 values are included to demonstrate the degree of linearity.

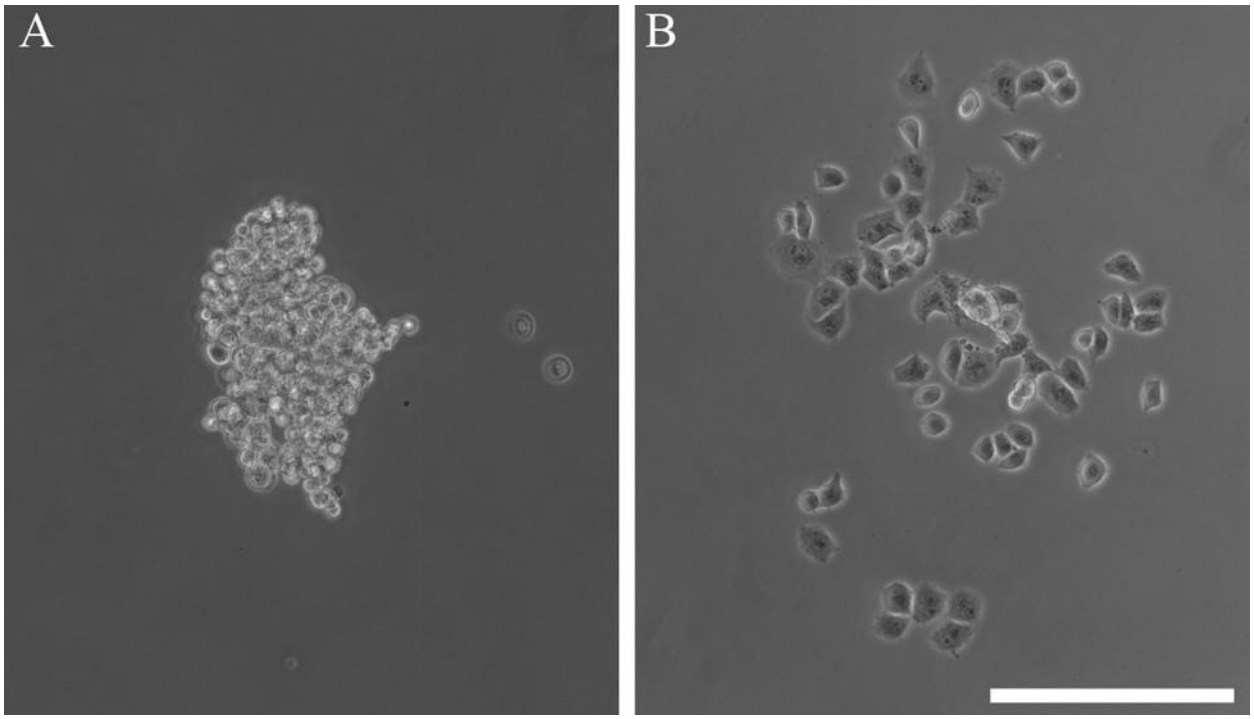

Supplemental Figure 5 - CMD is non-toxic to PANC-1 cells. ***A*****:** PANC-1 cells were cultured on CMD for 3 days, which formed small aggregates without attachment to the CMD surface. ***B*****:** PANC-1 aggregates initially cultured above the CMD surface for 3 days were passaged onto normal culture surfaces, which allowed binding and proliferation. Bar = 250 μm.

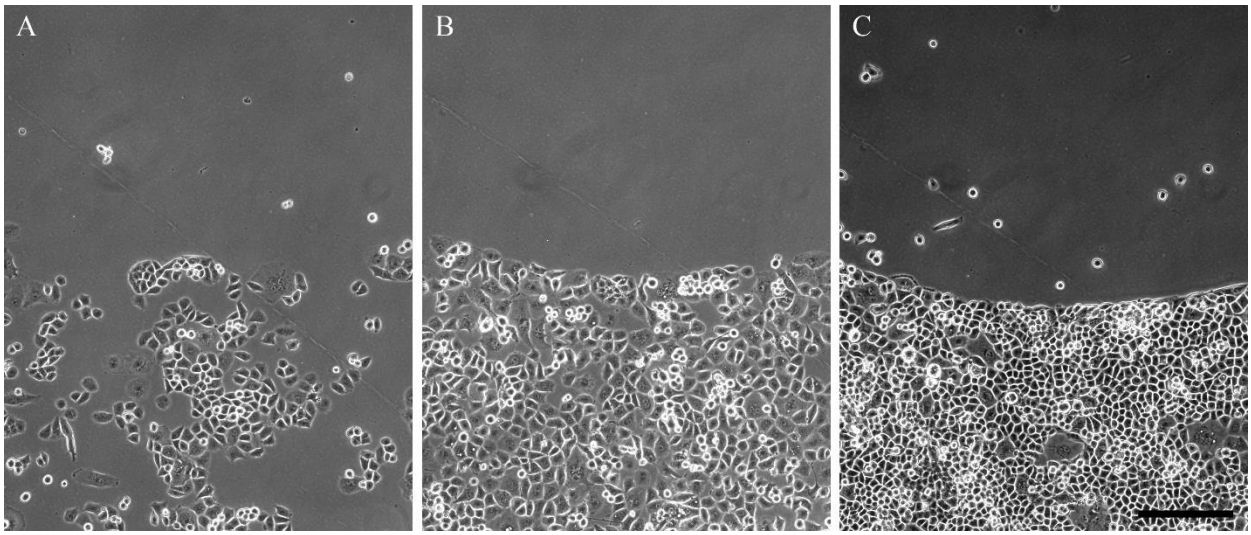

Supplemental Figure 6 - PANC-1 cells avoid growth onto CMD surfaces over an extended time. CMD was applied as a pattern (by applying 25 µL drops of poly-L-lysine as the CMD attachment substrate) and near identical fields of view were identified by surface blemishes, in this case a prominent diagonal line running from upper left to lower right, as well as smaller markings. ***A*:** Phase contrast image after 3 days of growth. ***B*:** Phase contrast image after 12 days of growth. ***C*:** Phase contrast image after 14 days of growth. Bar = 250 µm.

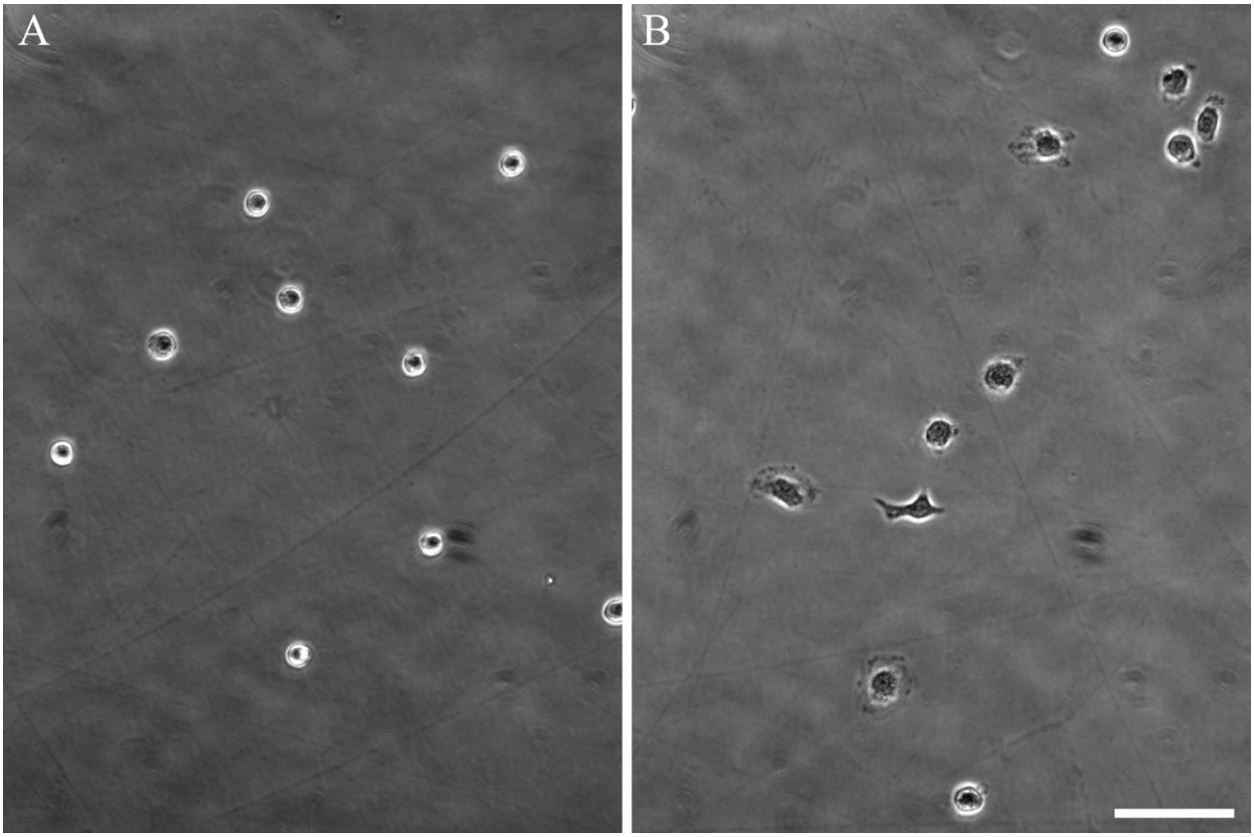

Supplemental Figure 7 - Peritoneal macrophages on CMD. Peritoneal macrophages were applied to surfaces for two hours, after which they were rinsed to remove non-attached material, and photographed. ***A*:** Phase contrast image of macrophages on culture surface without CMD (CMD was applied, but without the pre-application of poly-L-lysine). ***B*:** Phase contrast image of macrophages on CMD. Bar = 50 μm. To prepare peritoneal macrophage cultures, the mouse peritoneal cavity was first flushed with islet growth medium which was collected, centrifuged at 1000 rpm for five minutes and the resulting cell pellet seeded onto culture plates bearing CMD or control plates (CMD applied with poly-L-lysine omitted). Cultures were washed with culture medium after 2 hours to remove non-adherent cells and imaged.

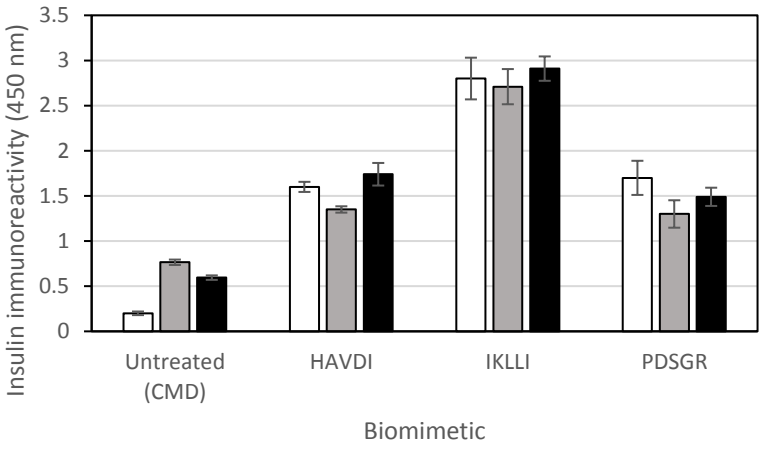

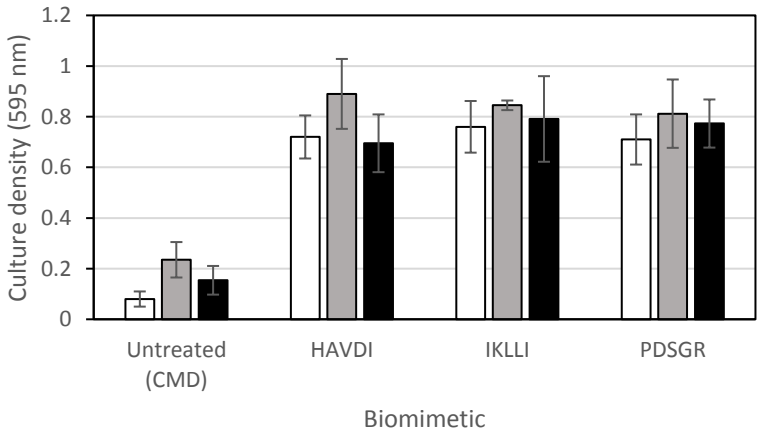

Supplemental Figure 8 - Insulin content of INS-1 cells on biomimetic surfaces. The upper panel represents insulin content as measured by cell-ELISA. The lower panel represents culture densities as determined by the Janus Green B assay. Each bar color represents the averages of three individual experiments to demonstrate variation between islet preparations. Error bars indicate standard deviations between three wells in each experiment.

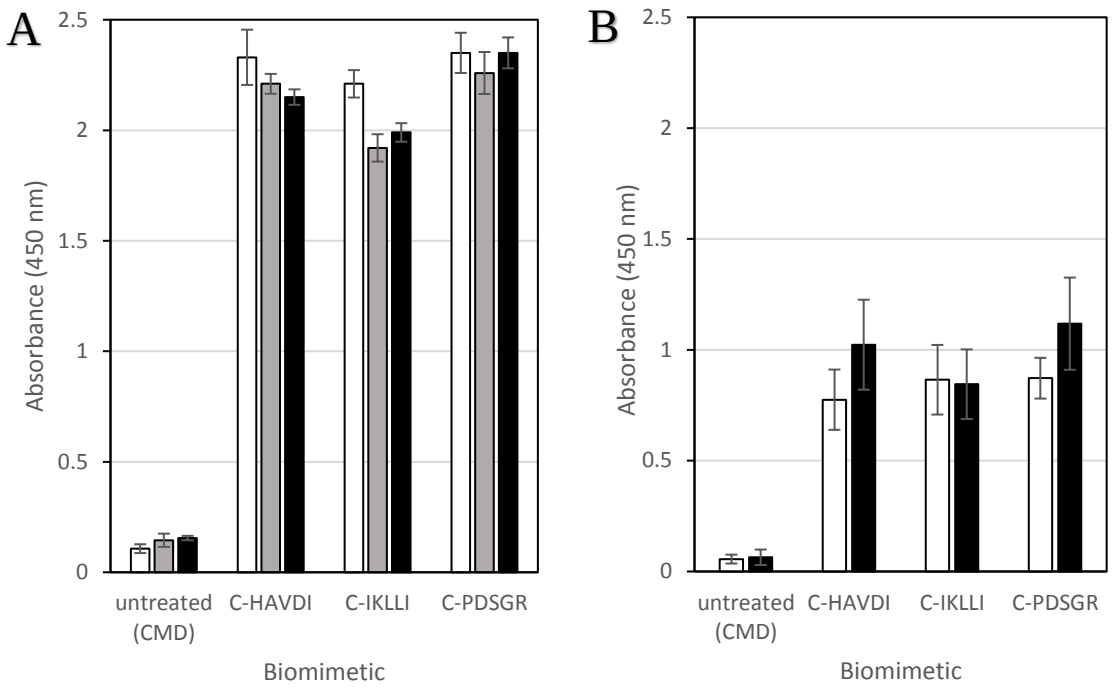

Supplemental Figure 9 - Insulin content of cultures on C-terminal (cysteine-linked) biomimetic surfaces. *A*: Insulin content of INS-1 cells cultured for 5 days on the indicated biomimetic surfaces. ***B*:** Insulin content of Accutase®-dissociated islets cultured for 5 days on the indicated biomimetic surfaces. Each bar color represents the averages of three individual experiments to demonstrate variation between islet preparations. Error bars indicate standard deviations between three wells in each experiment.

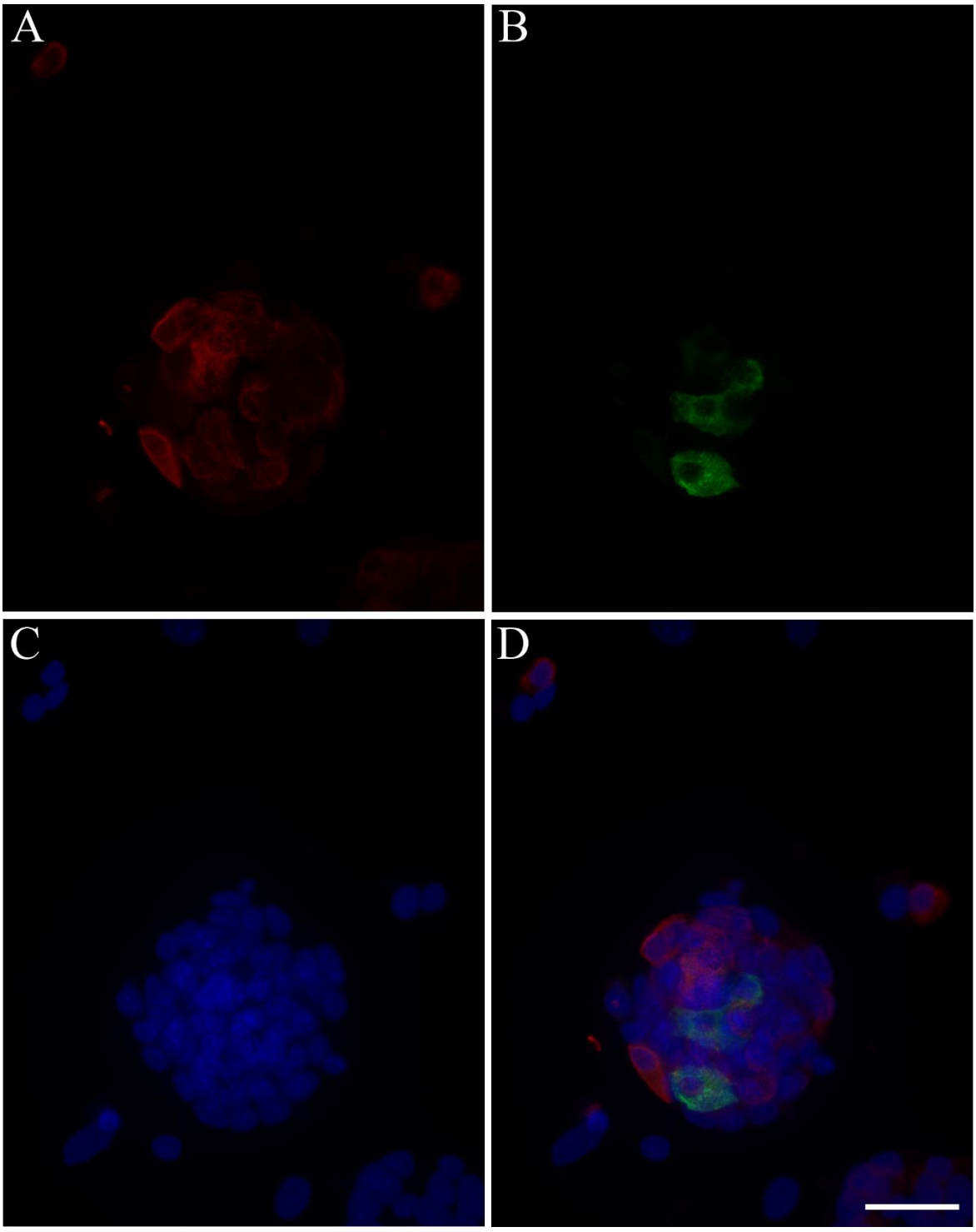

Supplemental Figure 10 - Immunocytochemistry of cultured islet cells on HAVDI-biomimetic. Accutase®-dissociated islets were cultured on the HAVDI-biomimetic surface for 9 days and processed for immunochemistry. ***A*:** Anti-insulin staining (red). ***B*:** Anti-glucagon staining (green). ***C*:** Hoechst staining nuclei (blue). ***D*:** Merge of the three color channels. Bar = 10 μm.